

# Computation of thermal conductivity based on Path Integral Monte Carlo methods

Vladislav Efremkin,<sup>1</sup> Stefano Mossa,<sup>2</sup> Jean-Louis Barrat,<sup>3,4</sup> and Markus Holzmann<sup>5,4</sup>

<sup>1</sup>Center for Advanced Systems Understanding, Helmholtz Zentrum Dresden-Rossendorf, D-02826 Görlitz, Germany

<sup>2</sup>Université Grenoble Alpes, CEA, IRIG-MEM-LSim, 38054 Grenoble, France

<sup>3</sup>Univ. Grenoble Alpes, CNRS, LIPhy, 38000 Grenoble, France

<sup>4</sup>Institut Laue Langevin, 38000 Grenoble, France

<sup>5</sup>Univ. Grenoble Alpes, CNRS, LPMMC, 38000 Grenoble, France

(Dated: February 19, 2026)

The calculation of thermal conductivity in insulating solids at temperatures below the Debye temperature is problematic, due to the breakdown of classical and semi-classical approaches. In this work, we present a fully quantum methodology to compute thermal conductivity based on Path Integral Monte Carlo (PIMC) simulations combined with the Green–Kubo linear response theory. The method is applied to crystalline argon modeled by a Lennard-Jones potential, a paradigmatic system where quantum effects strongly affect both thermodynamic and transport properties. From PIMC simulations, we obtain the temperature-dependent phonon frequencies, lifetimes, and specific heat. From the imaginary time correlations of the energy current, we extract the thermal transport coefficients based on a physically motivated prior. We show that the experimentally observed increase of the thermal conductivity at low temperatures cannot be explained within a standard Peierls–Boltzmann framework or quasi-harmonic approximation using phonon lifetimes alone. Instead, a distinct transport lifetime emerges from the analysis of heat-current correlations. Our results demonstrate that quantum Monte Carlo methods provide a robust, non-perturbative framework to investigate heat transport in insulating solids, beyond the limits of classical molecular dynamics and quasi-harmonic approximations.

*Introduction.*– Heat transport is an important property of matter and is of major current interest, both theoretical and practical, in physics, chemistry, and materials science [1]. A heat flux  $\mathbf{J}$  occurs inside the bulk of the material in the presence of a temperature gradient,  $\nabla T$ . In the limit of small temperature gradients, Fourier’s law,

$$\mathbf{J} = -\underline{\kappa}\nabla T, \quad (1)$$

defines the heat conductivity tensor,  $\underline{\kappa}$ , at given thermodynamic state, *e. g.*, temperature and pressure/density.

The theory of heat conduction in crystalline solids has been established by Peierls a century ago [2]. First principle calculations of the thermal conductivity for molecular systems described by a model Hamiltonian,

$$H = \sum_i \frac{p_i^2}{2m} + \sum_{i<j} v(r_{ij}), \quad (2)$$

have been mostly based either on Molecular Dynamics (MD) calculations or lattice dynamics within the Boltzmann transport equation. Generalizations to amorphous and partially disordered systems based on Wigner’s dynamics or quasi-harmonic Green-Kubo (QHGK) framework were achieved more recently [3–8], but rely on a perturbative description in the anharmonicity.

So far, non-perturbative computational methods have been intrinsically based on classical or semi-classical dynamics. Their reliability for temperatures significantly below the Debye temperature,  $T_D$ , is thus highly questionable, as they either completely fail to reproduce the expected drop of the specific heat, or incorporate this feature purely phenomenologically. Although classical MD calculations for solid argon lead to surprisingly good

agreement with experiment down to low  $T$ , any attempt to empirically include quantum effects to describe the observed heat capacity has degraded the apparent agreement, and has also failed to reproduce the sharp increase of the heat conductivity observed at low temperatures [9].

Here, we employ Path Integral Monte Carlo (PIMC) methods [10] to overcome these limitations. We calculate the heat conductivity within the Green-Kubo linear response theory, based on a simple yet robust physical model underlying the spectral reconstruction of the imaginary time current-current correlations. Our approach fully accounts for anharmonic and quantum effects, without relying on any perturbative expansion. Focusing on a Lennard-Jones (LJ) model system with parameters calibrated for solid argon (Ar), we show that it quantitatively captures the steep increase of thermal conductivity on lowering temperature below the Debye temperature, a phenomenon not described by QHGK approximations. Note that our methodology does not rely on the presence of perfect crystalline structures, and can therefore be applied to any localized systems, *e. g.*, disordered or amorphous solids. In particular, similar to the crystalline Ar discussed below, accessible imaginary-time correlation functions also enable to directly test and verify spectral functions of the harmonic [11, 12] or QHGK theory [13] for the glass state, and naturally extend them into the quantum regime.

*Theory.*– Based on Green-Kubo linear response, the thermal conductivity can be obtained at thermodynamic equilibrium from the energy-current correlation function as,

$$\kappa = \frac{1}{3} \text{Tr} \underline{\kappa} = \frac{k_B \beta^2}{3} \sum_{\alpha} \lim_{\omega \rightarrow 0} \Lambda_{\alpha\alpha}(\omega). \quad (3)$$

Here,  $\beta = 1/k_B T$  is the inverse temperature, and

$$\begin{aligned}\Lambda_{\alpha\alpha}(\omega) &= \frac{1}{V} \lim_{\eta \rightarrow 0^+} \Re \int_0^\infty dt e^{i(\omega+i\eta)t} \langle J_\alpha(t) J_\alpha(0) \rangle \quad (4) \\ &= \frac{\pi}{V} \sum_{n,m} \frac{e^{-\beta E_n}}{Z} |\langle E_n | J_\alpha | E_m \rangle|^2 \delta(\omega - E_{mn}),\end{aligned}$$

where  $|E_n\rangle$  is an energy eigenstate of energy  $E_n$ ,  $Z = \text{Tr} e^{-\beta H}$ ,  $E_{mn} = E_m - E_n$ ,  $V$  is the system volume, and the  $J_\alpha$  are the  $\alpha = x, y, z$  components of the heat current operator,  $\mathbf{J}$ , to be discussed below.

Within numerical Path Integral Monte Carlo (PIMC) or Molecular Dynamics (PIMD) methods, we are able to compute imaginary time,  $\tau$ , correlation functions controlling both systematic and statistical bias, as,

$$\begin{aligned}C_{\alpha\alpha}(\tau) &= \frac{1}{V} \langle J_\alpha(\tau) J_\alpha(0) \rangle \quad (5) \\ &\equiv \frac{1}{ZV} \text{Tr} \left[ e^{-(\beta-\tau)H} J_\alpha e^{-\tau H} J_\alpha \right],\end{aligned}$$

which implicitly provides  $\Lambda_{\alpha\alpha}(\omega)$  using,

$$C_{\alpha\alpha}(\tau) = \frac{1}{\pi} \int_0^\infty d\omega \Lambda_{\alpha\alpha}(\omega) \left[ e^{-\tau\hbar\omega} + e^{-(\beta-\tau)\hbar\omega} \right], \quad (6)$$

as can be checked by explicit insertion of the respective spectral representations.

Dynamics at temperatures far below melting is usually dominated by normal mode vibrations (phonons in crystals), obtained from an an effective potential energy arising for the deviations from the equilibrium sites. In the harmonic approximation, this effective potential energy is approximated by a quadratic form in the lattice displacements  $\mathbf{u}_i = \mathbf{r}_i - \mathbf{R}_i$ ,

$$V_h = \frac{1}{2} \sum_{i\alpha j\beta} u_{i\alpha} D_{i\alpha, j\beta} u_{j\beta}. \quad (7)$$

For classical systems at low  $T$ , the effective force constants,  $D_{i\alpha, j\beta}$ , are given by the Hessian of the total potential energy, and the eigenmodes  $\{e_n^{i\alpha}\}$  of the dynamical matrix,  $\sum_{j\beta} D_{i\alpha, j\beta} e_n^{j\beta} = m\omega_n^2 e_n^{i\alpha}$ , determine the phonon frequencies  $\omega_n$ . (Here,  $m$  is the mass.) Anharmonic and quantum effects introduce an effective temperature and density dependence. In particular, quantum corrections reduce the modal heat capacity,  $c_n = k_B (\hbar\omega_n/k_B T)^2 e^{\hbar\omega_n/k_B T} / (e^{\hbar\omega_n/k_B T} - 1)^2$  compared to the classical values, and, within an effective harmonic theory, we have  $C_V^h = \sum_n c_n$ .

Phonons in the harmonic approximation usually provide a reliable quantitative description of specific heat measurements, including the Debye  $\propto T^3$  dependence at low  $T$ . In this regime, one expects the heat current to also be well described using its harmonic approximation,

$$\mathbf{J}^h = \frac{1}{2} \sum_{i\alpha j\beta} (\mathbf{R}_i - \mathbf{R}_j) D_{i\alpha, j\beta} u_{i\alpha} p_{j\beta} / m, \quad (8)$$

with  $p_{j\beta}$  the momenta. (See End Matter for the full current expression.) In the following we focus on the harmonic current-current correlation functions,

$$C_{\alpha\alpha}^h(\tau) = \langle J_\alpha^h(\tau) J_\alpha^h(0) \rangle / V. \quad (9)$$

For an ideal harmonic crystal, where we neglect any anharmonic effect in the imaginary time evolution, the corresponding spectral density for  $\omega > 0$  can be written as the sum of a singular part,  $\Lambda_\alpha^s(\omega, \Gamma \rightarrow 0)$ , which develops a delta function at zero frequency, and a regular part,  $\Lambda_\alpha^r(\omega, \Gamma \rightarrow 0)$ , which does not contribute for  $\omega \rightarrow 0$ , *i. e.*,

$$\Lambda_{\alpha\alpha}^{h,0}(\omega) = \Lambda_\alpha^s(\omega, \Gamma \rightarrow 0) + \Lambda_\alpha^r(\omega, \Gamma \rightarrow 0). \quad (10)$$

Here,  $\Gamma$  refers generically to a damping mechanism of the harmonic modes, which vanishes in the harmonic limit [13], and is sometimes used as an adjustable parameter [11]. Introducing the decomposition of the harmonic current in normal modes, we obtain,

$$\begin{aligned}\Lambda_\alpha^s(\omega, \Gamma) &= \frac{1}{V} \sum_{nm} (\nu_{nm}^\alpha)^2 \frac{\hbar\omega_n}{e^{\beta\omega_n} - 1} \frac{\hbar\omega_m}{1 - e^{-\beta\omega_m}} \quad (11) \\ &\times \frac{(\omega_n + \omega_m)^2}{4\omega_n\omega_m} \frac{\Gamma_{nm}}{(\omega - \omega_m + \omega_n)^2 + \Gamma_{nm}^2} \\ \Lambda_\alpha^r(\omega, \Gamma) &= \frac{1}{8V} \sum_{nm} (\nu_{nm}^\alpha)^2 \frac{\hbar\omega_n}{1 - e^{-\beta\omega_n}} \frac{\hbar\omega_m}{1 - e^{-\beta\omega_m}} \quad (12) \\ &\times \frac{(\omega_n - \omega_m)^2}{2\omega_n\omega_m} \frac{\Gamma_{nm}}{(\omega - \omega_n - \omega_m)^2 + \Gamma_{nm}^2},\end{aligned}$$

with,

$$\nu_{nm}^\alpha = \frac{1}{2\sqrt{\omega_n\omega_m}} \sum_{i\beta j\gamma} e_{i\beta}^n D_{i\beta j\gamma} e_{j\gamma}^m (\mathbf{R}_{i\alpha} - \mathbf{R}_{j\alpha}). \quad (13)$$

In the QHGK approximation for the thermal conductivity [3], the broadening  $\Gamma_{nm} \simeq \Gamma_n^{ph} + \Gamma_m^{ph}$  is given by the inverse phonon lifetimes,  $\Gamma_n^{ph}$ , determined numerically from the anharmonic (cubic) terms of the energy employing the Fermi's golden rule.

In a perfect crystal, the matrix elements  $\nu_{nm}^\alpha$  of Eq. (13) essentially reduce to the group velocity [14],  $v_{\mathbf{k}\alpha} = \partial\omega_{\mathbf{k}\alpha}/\partial\mathbf{k}$ , which is diagonal in momentum space. We, therefore, recover the Peierls-Boltzmann form of the thermal conductivity,

$$\kappa_{PB} = \frac{k_B}{V} \sum_{\mathbf{k}\alpha} c_{\mathbf{k}\alpha} v_{\mathbf{k}\alpha}^2 \tau_{\mathbf{k}\alpha}. \quad (14)$$

Here,  $c_{\mathbf{k}\alpha}$  is the modal specific heat, and the lifetimes  $\tau_{\mathbf{k}\alpha}$  are provided by the phonon lifetimes,  $\tau_{\mathbf{k}\alpha}^{ph} = 1/2\Gamma_{\mathbf{k}\alpha}^{ph}$  in the QHGK approach [3]. In general, however, one expects vertex corrections beyond the quasi-harmonic Green-Kubo approach [7] leading to transport lifetimes,  $\tau_{\mathbf{k}\alpha}^{tr}$ , which may differ from the bare phonon ones, in particular for temperatures below  $T_D$ . The goal of the PIMC calculations we describe below is to naturally take into

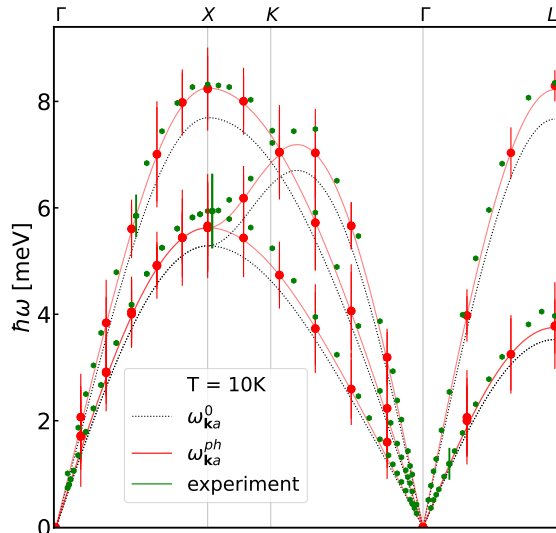


Figure 1. Phonon dispersion relationship,  $\omega_{\mathbf{k}a}$  for solid argon, along the indicated directions of the wave-vector,  $\mathbf{k}$ . The results for longitudinal ( $a = L$ ) and transverse ( $a = T$ ) phonons,  $\omega_{\mathbf{k}a}^{ph}$  (red circles) obtained from the normal modes correlation function for a simulated system with  $N = 864$  atoms are compared with experimental data [15]. The grey dotted lines indicate the harmonic frequencies,  $\omega_{\mathbf{k}a}^0$ , pertaining to the ideal harmonic crystal. The vertical (red) bars quantify the broadening of the phonon lines due to their finite lifetimes,  $\tau_{\mathbf{k}a}^{ph}$ . The experimental line-width [15] is also indicated as a vertical (green) bar, for selected data points.

account all quantum and anharmonic effects, in a non-perturbative manner.

Path Integral Monte Carlo methods enable the computation of equilibrium observables, including imaginary time correlation functions [10]. From the current-current correlation function in imaginary time, Eq. (5),  $\Lambda_{\alpha\alpha}(\omega)$  can be obtained by inverting Eq. (6). Such an analytical continuation is strongly affected by the stochastic error of  $C_{\alpha\alpha}(\tau)$ , intrinsic to any Monte Carlo method, but sufficiently robust results can be obtained [16]. Validation of reconstructed density of states on independent data, as proposed in [17], reduces reliance on model assumptions, and provides objectives comparisons.

Although a straightforward PIMC estimator for the harmonic heat flux operator, Eq. (8), can be obtained by direct application of the momentum operator on the discretized path, it suffers from large variance, which diverges in the limit of vanishing imaginary time discretization, similar to the case of the direct kinetic energy estimator [10]. We therefore use a variance-reduced *virial* estimator, as given in [17, 18], essential for the accurate determination of current-current correlation functions.

*Results.*— We now apply the methodology outlined above to crystalline argon, modeled by a LJ poten-

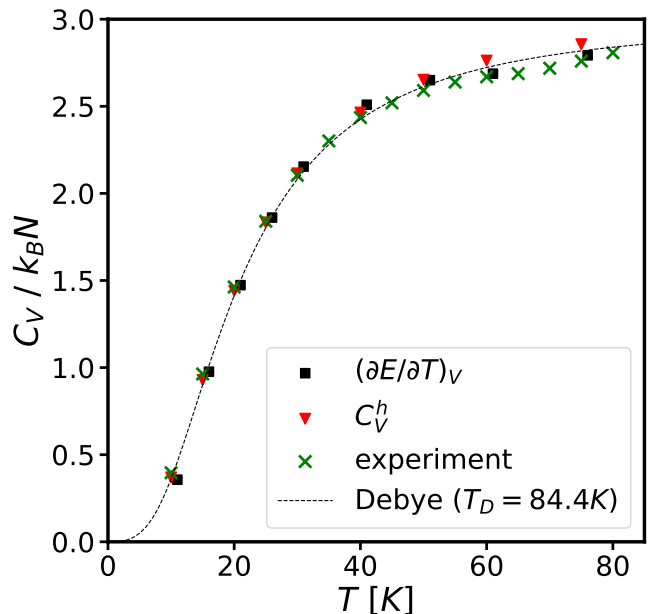


Figure 2. Specific heat of solid argon from PIMC calculations compared to the experimental results. The black squares are obtained from the numerical derivative of the total energy, whereas  $C_V^h$  (triangles) is the specific heat determined in the harmonic approximation based on the phonon frequencies,  $\omega_{\mathbf{k}a}^{ph}$ , obtained from the normal mode correlation functions. The experimental data from [19] ( $\times$ ) are also shown for comparison, together with the corresponding values predicted by the Debye model with  $T_D = 84.4$  K (dashed line).

tial,  $v(r) = 4\epsilon [(r/\sigma)^{-12} - (\sigma/r)^{-6}]$ , with  $\epsilon = 119.8$  K,  $\sigma = 3.405$  Å [20], and a cutoff distance,  $r_c = 2.5\sigma$ . Unless explicitly stated, results are reported in LJ units, where time is expressed in units of  $t_0^{Ar} = 2.16 \times 10^{-12}$  s, and the strength of quantum effects is encoded in the dimensionless parameter  $Q = \sqrt{\hbar^2/m\sigma^2\epsilon} \simeq 0.0296$ . Below  $T \approx 75$  K, and close to ambient pressure, the atoms arrange in a fcc lattice. Our PIMC simulations are performed in the (NVT) ensemble, at densities  $\rho = N/V$  varying from  $\rho\sigma^3 = 1.052$  at 10 K to 0.98 at 75 K, approximately following the  $P = 0$  isobar, with an imaginary time step discretization based on the primitive approximation [10] corresponding to a temperature  $\approx 2000$  K. Below, we primarily present the results of computations with  $N = 108$ , as we have not observed essential differences compared to larger systems with  $N = 864$ . Note that here we do not particularly focus on precise quantitative modelling of experiments, the case of argon serving as a first proof of concept.

We start by extracting the effective phonon frequencies and lifetimes from the spectra associated with the imaginary time correlation functions of the phonon modes,

$$\langle q_{\mathbf{k}a}(\tau)q_{\mathbf{k}a}(0) \rangle = \int_0^\infty d\omega S_{\mathbf{k}a}(\omega) [e^{-\tau\hbar\omega} + e^{-(\beta-\tau)\hbar\omega}]. \quad (15)$$

Here, the  $q_{\mathbf{k}a}$  are the normal mode coordinates which

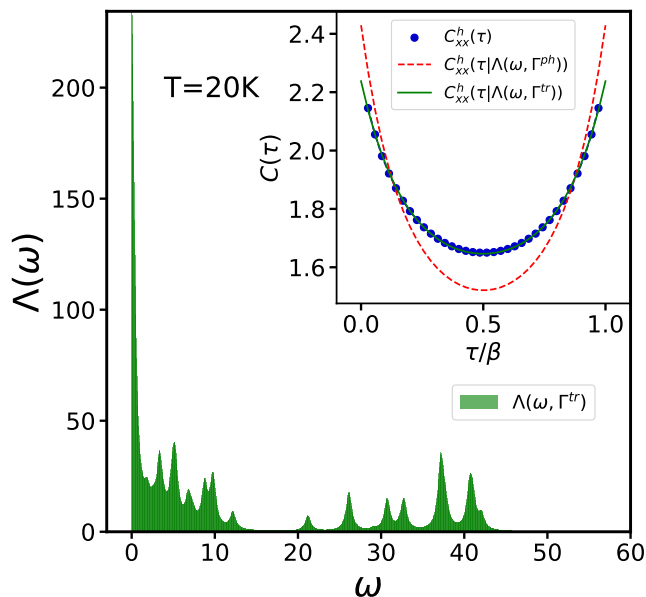


Figure 3. *Main panel:* Spectral function of the harmonic current correlations at  $T = 20\text{K}$ . *Inset:* The corresponding imaginary time correlations  $C_{xx}^h(\tau)$ , obtained from PIMC (circles) together with the reconstructed one,  $C_{xx}^h(\tau|\Lambda)$ , based on the prior  $\Lambda(\omega, \Gamma^{tr})$ , determining the inverse transport lifetime  $\Gamma^{tr}$  (solid line). For comparison, we also show the best reconstruction obtained by imposing the inverse phonon lifetime,  $C_{xx}^h(\tau|\Lambda(\omega, \Gamma^{ph}))$  (dashed line), incompatible with the calculated imaginary time correlation.

diagonalize the Hessian matrix of the Lennard-Jones interaction,  $\mathbf{k}$  is the wave vector, and  $a$  the (longitudinal or transverse) polarization. Assuming a Lorentzian distribution for the spectral function,  $S_n(\omega)$ , we determine the effective phonon frequencies,  $\omega_{\mathbf{k}a}^{ph}$ , and lifetimes,  $\tau_{\mathbf{k}a}^{ph}$ , from the reconstruction of the phonons imaginary time correlations. In Fig. 1 we compare the resulting phonon dispersion to the experiments of [15], at  $T = 10\text{K}$ . We observe an approximately 5% shift compared to the bare (unperturbed) frequencies,  $\omega_{\mathbf{k}a}^0$ , computed from diagonalizing the Hessian of the LJ potential, which is in reasonable agreement with inelastic neutron scattering data. The obtained phonon lifetimes are also compatible with the experimental line-widths reported in [15].

From our PIMC calculations we further have direct access to the temperature dependence of the total energy. In Fig. 2 we compare the resulting specific heat with experimental data [19], together with the harmonic approximation based on the phonon frequencies,  $\omega_{\mathbf{k}a}^{ph}$ , and bare phonons,  $\omega_{\mathbf{k}a}^0$ . Clearly, an effective harmonic model based on the exact phonon frequencies provides a quantitative description for the specific heat, systematically improving the predictions based on bare frequencies (see Supplemental Material). Approaching the Debye temperature, deviations become visible, presumably due to stronger anharmonic effects which are not accurately grasped by an effective harmonic theory.

From the phonon mode correlation functions (15), we next determine a mean phonon lifetime,  $\tau^{ph}$ , averaged over the first Brillouin zone. Based on the calculated phonon frequencies, we can directly estimate the heat conductivity from the Peierls-Boltzmann equation, Eq. (14), which corresponds to the QHGK approximation for the considered perfect crystal. As shown in Fig. 4, this approximation qualitatively fails to reproduce the steep increase of the thermal conductivity at temperatures below  $T_D$ . The behavior is actually similar to the results extracted from out-of equilibrium MD which heuristically include quantum effects for phonons to reproduce the drop of the specific heat, see [9]. The disagreement with experiment cannot thus be attributed to a failure of the determination of phonon frequencies and lifetimes, but instead points to a transport lifetime which becomes significantly different from  $\tau_{\mathbf{k}a}^{ph}$  upon lowering  $T$ .

To move beyond the QHGK approximation and the related Peierls approximation, we now analyze the correlation functions of the harmonic current  $C_{\alpha\alpha}^h(\tau)$  of Eq. (9), in order to reconstruct the spectral density. Instead of attempting a purely numerical inversion [16, 21], we maximally constrain the prior model based on the following physical considerations. First, from the spectral analysis of the phonon correlation functions we have determined phonon frequencies,  $\omega_{\mathbf{k}a}^{ph}$ , which provide an accurate description of the static energy fluctuations, as confirmed from the specific heat comparisons. As a consequence, it is justified to expect that the heat currents in the harmonic approximation will also provide an accurate description of thermal transport.

Second, the spectra of the harmonic current-current correlation function, should be satisfyingly close to the ideal harmonic spectra based on the extracted phonon frequencies. Note that the phonon frequencies already contain a temperature dependent anharmonicity shift of  $\omega_{\mathbf{k}a}^0$ . In order to take into account broadening associated to anharmonicity, we expect the low frequency spectra to be well described by  $\Lambda_{\alpha}^s(\omega, \Gamma^{tr})$ , where  $\Gamma^{tr}$  is a broadening that may differ from the (mean) phonon lifetime  $\Gamma^{ph}$ . Since the detailed modifications of the regular part are beyond the scope of the present work, our prior  $\Lambda(\omega, \Gamma) \equiv \Lambda_{\alpha}^s(\omega, \Gamma) + \xi \Lambda_{\alpha}^r(\omega, \Gamma)$ , using a mode independent broadening, describes the simplest model suitable for our purpose, as will be seen below. Indeed, we have found that the two parameters  $\Gamma(T)$  and  $\xi(T)$ , at each temperature, are sufficient for a quantitative reconstruction of the imaginary time correlations in the entire temperature range from  $T = 15\text{K}$  to melting (see Supplemental Material).

In Fig. 3 we illustrate the sensitivity to  $\Gamma$ , by comparing the best reconstruction obtained by fixing  $\Gamma$  to the mean phonon lifetime  $\Gamma^{ph}$ , with the optimal solution yielding  $\Gamma^{tr}$ . In Fig. 4 we show the resulting thermal conductivity obtained from our reconstruction, which closely follows the experimental values, in particular the rapid increase at lower temperatures, which is not captured by the use of phonon lifetimes in the Peierls-Boltzmann

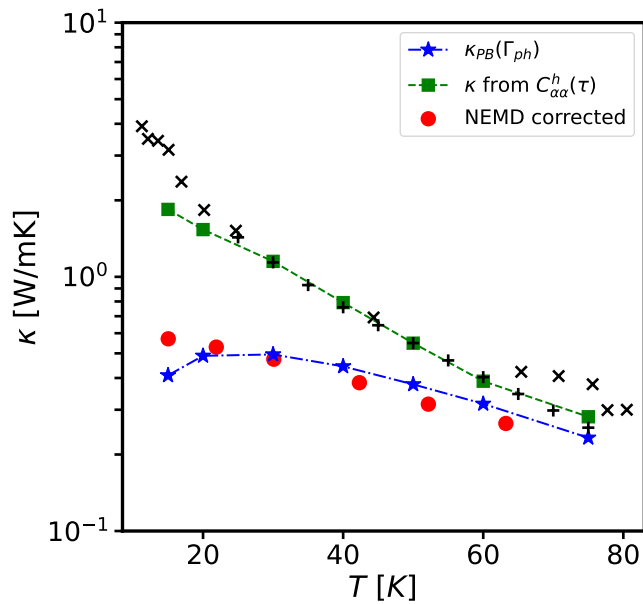


Figure 4. Thermal conductivity of solid argon obtained from the spectral reconstruction of  $C_{xx}(\tau)$ , compared with the result of the Peierls-Boltzmann equation,  $\kappa_{BP}$  of Eq. (14), based on the PIMC phonon frequencies and lifetimes. The red circles are results from the NEMD calculations reported in [9]. The experimental data from [22] and [23] are indicated in black as  $\times$  and  $+$ , respectively.

equation.

*Conclusions.*— In this work, we have introduced a general methodology for calculating the thermal conductivity of insulating solids, making maximal use of the information obtained from equilibrium PIMC calculations. The PIMC simulations allow us to obtain in a non-perturbative manner the effective vibrational density of states. This information is used to build a reasonable prior *ansatz* for the heat current correlation function. The latter is next used to effectively invert the imaginary time correlation function, eventually giving access to the spectral density. Our calculations for solid argon show that the method leads to results consistent with experiment, and that the rise of the thermal conductivity at low temperatures is basically due to a transport lifetime which differs from the phonon lifetime obtained from normal mode analysis, as single phonon scattering does not lead to a full decorrelation of the heat current. Our method provides a computational framework for calculating heat transport in insulating solids within Path Integral Monte Carlo or Path Integral Molecular Dynamics methods. Although here we have focused on a perfect, simple crystal, our approach directly extends to more complex crystals or amorphous systems, where it should provide a definitive assessment of the role and importance of quantum effects at low temperatures [24–26].

*Acknowledgements.*— This work was supported by the project Heatflow (Grant No. ANR-18-CE30-0019) funded by the French national funding agency, Agence

Nationale de la Recherche.

## END MATTER

*Total current.*— Within PIMC, it is straightforward to go beyond the harmonic approximation of the energy current and use the total energy current,

$$\mathbf{J} = \frac{1}{2} \sum_{i \neq j} (\mathbf{R}_i - \mathbf{R}_j) [\mathbf{f}_{ij} \cdot (\mathbf{p}_i/m - \mathbf{u})] \quad (16)$$

where  $\mathbf{f}_{ij} = -\nabla_i v(r_{ij})$  and we have subtracted the center of mass velocity,  $\mathbf{u} = \sum_i \mathbf{p}_i/Nm$ , to eliminate any spurious contributions due to the center of mass motion. We can then access and analyse the total current-current correlation function following exactly the same methodology as for the harmonic one.

However, in contrast to the harmonic current, the total current also contains higher order phonon transitions, affecting primarily the regular part of the spectral function, particularly visible in the correlations at short imaginary times. For a proper reconstruction, we have to include spectral weight,  $\tilde{\Lambda}(\omega)$ , at higher frequencies, to account for higher order transitions needed to for the reconstruction of the full current correlations in imaginary time. Since we do not expect these multi-phonon processes to modify significantly the singular part already

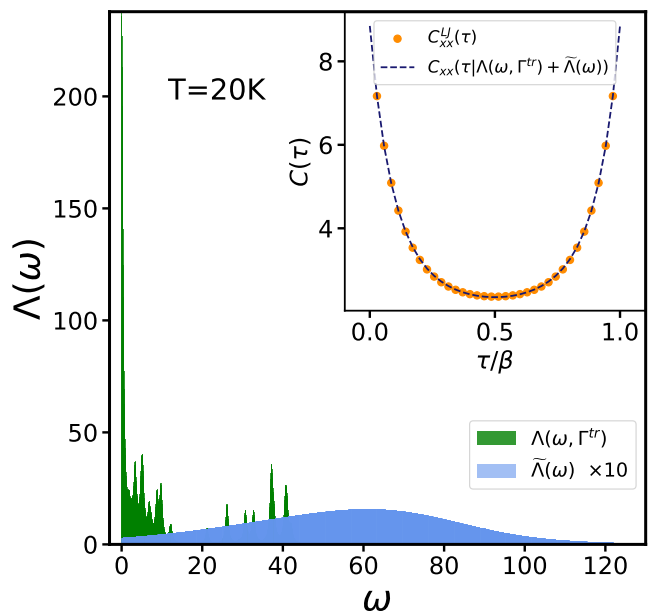


Figure 5. Spectral function of total current current correlations at  $T = 20\text{K}$ , based on the corresponding reconstruction  $\Lambda(\omega, \Gamma^{tr})$  of the harmonic current correlations and the additional spectral weight  $\tilde{\Lambda}(\omega)$ . Notice the difference in scale between the two components of the spectral density. The inset shows the reconstructed imaginary time correlation function of the total current obtained by optimizing only the additional weight  $\tilde{\Lambda}(\omega)$  without modifying  $\Lambda(\omega, \Gamma^{tr})$ .

contained in the harmonic current expression, we can account for the difference by assuming a smooth density of states at the scale of typical phonon frequencies. Therefore, we can reconstruct the difference of the density of states,  $\tilde{\Lambda}(\omega)$ , by using conventional maximum entropy methods [16, 17, 21].

In Fig. 5 we show the obtained spectral reconstruction from the prior  $\Lambda(\omega, \Gamma^{tr}) + \tilde{\Lambda}(\omega)$ . Here,  $\tilde{\Lambda}(\omega)$  is represented by a superposition of several Gaussians whose parameters are determined to reconstruct the imaginary time correlation function of the total current, whereas

$\Lambda(\omega, \Gamma^{tr})$  is given by the unmodified reconstruction of the corresponding harmonic current correlations. As expected, the total current correlations contain higher frequency components, but with an order of magnitude smaller intensity. Even though entropy effects of this unconstrained reconstruction is likely smearing out sharp features, the additional spectral weight close to  $\omega = 0$  is too small to modify significantly the value of the thermal conductivity. Within our precision, the thermal conductivity is quantitatively contained by the harmonic current correlations.

- 
- [1] N. W. Ashcroft and N. D. Mermin, *Solid State Physics* (Holt, Rinehart and Winston, New York, 1976).
- [2] R. Peierls, Zur kinetischen theorie der wärmeleitung in kristallen, *Annalen der Physik* **395**, 1055 (1929).
- [3] L. Isaeva, G. Barbalinardo, D. Donadio, and S. Baroni, Modeling heat transport in crystals and glasses from a unified lattice-dynamical approach, *Nature Comm.* **10**, 3853 (2019).
- [4] M. Simoncelli, N. Marzari, and F. Mauri, Unified theory of thermal transport in crystals and glasses, *Nature Physics* **15**, 809–813 (2019).
- [5] G. Barbalinardo, Z. Chen, N. W. Lundgren, and D. Donadio, Efficient anharmonic lattice dynamics calculations of thermal transport in crystalline and disordered solids, *Journal of Applied Physics* **128**, 135104 (2020).
- [6] M. Simoncelli, N. Marzari, and F. Mauri, Wigner formulation of thermal transport in solids, *Phys. Rev. X* **12**, 041011 (2022).
- [7] G. Caldarelli, M. Simoncelli, N. Marzari, F. Mauri, and L. Benfatto, Many-body green’s function approach to lattice thermal transport, *Phys. Rev. B* **106**, 024312 (2022).
- [8] A. Fiorentino and S. Baroni, From green-kubo to the full boltzmann kinetic approach to heat transport in crystals and glasses, *Phys. Rev. B* **107**, 054311 (2023).
- [9] O. N. Bedoya-Martínez, J.-L. Barrat, and D. Rodney, Computation of the thermal conductivity using methods based on classical and quantum molecular dynamics, *Phys. Rev. B* **89**, 014303 (2014).
- [10] D. M. Ceperley, Path integrals in the theory of condensed helium, *Rev. Mod. Phys.* **67**, 279 (1995).
- [11] P. B. Allen and J. L. Feldman, Thermal conductivity of glasses: Theory and application to amorphous si, *Phys. Rev. Lett.* **62**, 645 (1989).
- [12] P. B. Allen and J. L. Feldman, Thermal conductivity of disordered harmonic solids, *Phys. Rev. B* **48**, 12581 (1993).
- [13] A. Fiorentino, E. Drigo, S. Baroni, and P. Pegolo, Unearthing the foundational role of anharmonicity in heat transport in glasses, *Phys. Rev. B* **109**, 224202 (2024).
- [14] R. J. Hardy, Energy-flux operator for a lattice, *Phys. Rev.* **132**, 168 (1963).
- [15] Y. Fujii, N. A. Lurie, R. Pynn, and G. Shirane, Inelastic neutron scattering from solid  $^{36}\text{Ar}$ , *Phys. Rev. B* **10**, 3647 (1974).
- [16] H. Shao and A. W. Sandvik, Progress on stochastic analytic continuation of quantum monte carlo data, *Physics Reports* **1003**, 1 (2023).
- [17] V. Efremkin, J.-L. Barrat, S. Mossa, and M. Holzmann, Time correlation functions for quantum systems: Validating bayesian approaches for harmonic oscillators and beyond, *The Journal of Chemical Physics* **155**, 134108 (2021).
- [18] G. Carleo, G. Boéris, M. Holzmann, and L. Sanchez-Palencia, Universal superfluid transition and transport properties of two-dimensional dirty bosons, *Phys. Rev. Lett.* **111**, 050406 (2013).
- [19] O. G. Peterson, D. N. Batchelder, and R. O. Simmons, Measurements of x-ray lattice constant, thermal expansivity, and isothermal compressibility of argon crystals, *Phys. Rev.* **150**, 703 (1966).
- [20] A. Cuccoli, A. Macchi, V. Tognetti, and R. Vaia, Monte carlo computations of the quantum kinetic energy of rare-gas solids, *Phys. Rev. B* **47**, 14923 (1993).
- [21] M. Jarrell and J. Gubernatis, Bayesian inference and the analytic continuation of imaginary-time quantum monte carlo data, *Physics Reports* **269**, 133 (1996).
- [22] D. K. Christen and G. L. Pollack, Thermal conductivity of solid argon, *Phys. Rev. B* **12**, 3380 (1975).
- [23] I. Krupskii and V. Manzhelii, Multiphonon interactions and the thermal conductivity of crystalline argon, krypton, and xenon, *Sov. Phys. JETP* **28**, 1097 (1969).
- [24] P.-F. Lory, S. Pailhès, V. M. Giordano, H. Euchner, H. D. Nguyen, R. Ramlau, H. Borrmann, M. Schmidt, M. Baitinger, M. Ikeda, *et al.*, Direct measurement of individual phonon lifetimes in the clathrate compound ba7.81ge40.67au5.33, *Nature communications* **8**, 491 (2017).
- [25] A. J. Leggett and D. C. Vural, “tunneling two-level systems” model of the low-temperature properties of glasses: Are “smoking-gun” tests possible?, *The Journal of Physical Chemistry B* **117**, 12966 (2013).
- [26] D. Khomenko, C. Scalliet, L. Berthier, D. R. Reichman, and F. Zamponi, Depletion of two-level systems in ultra-stable computer-generated glasses, *Phys. Rev. Lett.* **124**, 225901 (2020).